

Effects of methanol on crystallization of water in the deeply supercooled region

Ryutaro Souda

Nanoscale Materials Center, National Institute for Materials Science, 1-1 Namiki, Tsukuba, Ibaraki 305-0044, Japan

(Received 6 December 2006; published 30 May 2007)

The interaction of water with adsorbed methanol and butane is investigated and the crystallization mechanism of deeply supercooled water is discussed. Amorphous solid water becomes viscous liquid at temperatures greater than 136 K, and then a more fluidized liquid phase appears at 165 K, thereby engendering film dewetting. Crystallization occurs only in the dewetted films as revealed from the abrupt redshift and narrowing of the infrared absorption band. If methanol is incorporated in the bulk of water, crystallization occurs at lower temperatures (152 K) because water is nucleated by methanol. The crystallization in the viscous liquid phase ($136\text{ K} < T < 165\text{ K}$) is thought to be quenched without such nuclei, whereas spontaneous nucleation occurs in supercooled liquid water that appears at 165 K. The butane molecules, which are hydrated in the bulk of amorphous solid water, are released almost completely up to 165 K, although this dehydration channel is suppressed considerably if crystallization is induced by methanol. It is therefore suggested that butane dehydration is related to the phase transition of liquidlike water rather than crystallization.

DOI: [10.1103/PhysRevB.75.184116](https://doi.org/10.1103/PhysRevB.75.184116)

PACS number(s): 68.18.Jk, 64.70.Ja, 68.55.Ac, 64.70.Pf

I. INTRODUCTION

Anomalous properties of water, such as the density maximum at $T=4\text{ }^\circ\text{C}$, might be explained using the presence of two liquid phases. According to this second critical-point hypothesis,¹⁻³ it is important to uncover the properties of water in the deeply supercooled region because a distinct liquid phase is predicted to appear at ambient pressure. However, liquid water cannot be supercooled below 235 K because of homogeneous nucleation. Another route to supercooled liquid water is heating glassy water. The glassy water is prepared in three different ways: amorphous solid water (ASW) is formed by deposition of water vapor onto a cold substrate, hyperquenched glassy water (HGW) is vitrified liquid water at an extremely high rate of cooling, and low density amorphous (LDA) ice is prepared by pressure-induced amorphization of hexagonal ice followed by decompression and heating. Annealed ASW is structurally identical to HGW and LDA ice.⁴ Calorimetric studies of HGW indicate that the respective glass-transition temperature (T_g) and crystallization temperature (T_c) of water are 136 and 152 K, respectively.⁵⁻⁷ Recently, this assignment of T_g was questioned and subsequently reassigned to $165 \pm 5\text{ K}$.⁸⁻¹¹ The reassigned T_g appears to encounter a difficulty such that crystallization takes place prior to the glass-liquid transition. In reality, however, the crystallization rate increases at temperatures greater than 165–170 K following the onset at 152 K.^{5,6} This behavior has been attributed to two-step crystallization,⁷ but its origin remains unclear. The desorption rate of the water molecules has been shown to drop at 155–160 K in experiments of temperature programmed desorption (TPD),¹² together with the explosive desorption of the CCl_4 molecules embedded in the thick water films,¹³ which has been explained as being the result of ASW-film crystallization. In contrast, our results have revealed that the ASW film exhibits a very liquidlike nature in this temperature range:^{14,15} the self-diffusion of the water molecules commences at 136 K and then the film morphology changes abruptly at 165 K. Furthermore, an aqueous LiCl solution is

formed above 165 K when the ASW film is deposited on the polycrystalline LiCl film,¹⁶ indicating that the properties of liquidlike water change drastically at this temperature. The crystals are likely to grow in the liquid phase, but it remains unclear how the glass-liquid transition and crystallization of water are mutually related.

Additional insights into the properties of water may be gained from its ability to hydrate and dehydrate solute species. To date, we have reported that butane, which is incorporated in the bulk of the ASW film, is released up to 160–165 K,¹⁵ whereas methanol stays on the surface of the ASW film as a surfactant and suppresses its morphological change at 165 K.¹⁴ In this paper, we discuss the kinetics of the glass-liquid transition and the crystallization of water with and without the adsorbed butane and methanol molecules. The interactions of water with these molecules are investigated as a function of temperature using TPD, time-of-flight secondary ion mass spectrometry (TOF-SIMS), and reflection absorption infrared spectroscopy (RAIRS). Water crystallization can be studied from the shape change in the O-H stretch band of the water molecules.¹⁷⁻²¹ Particular attention is devoted to elucidating how the crystal growth and desorption kinetics of butane are affected by methanol adsorbed on the surface.

II. EXPERIMENT

The TOF-SIMS and TPD experiments were performed in an ultrahigh vacuum (UHV) chamber with base pressure of less than $1 \times 10^{-8}\text{ Pa}$, which was equipped with an electron-impact-type ion source, a linear TOF tube, a differentially pumped quadrupole mass analyzer for TPD, and a low-temperature sample stage cooled with a closed-cycle helium refrigerator. The TOF-SIMS measurement was made by bombarding a sample surface (floated with a bias voltage of +500 V) with a pulsed He^+ beam (2.0 keV, approximately 10 pA/cm^2). The positive ions, extracted through a grounded stainless-steel mesh (placed 4 mm above the sample surface), were detected using a channel electron multiplier. The

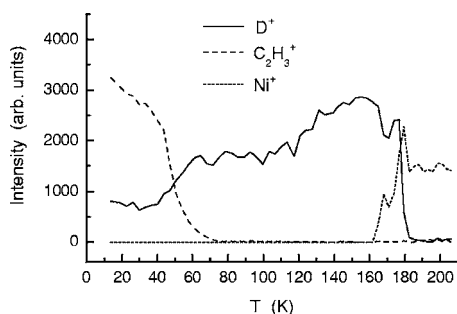


FIG. 1. TOF-SIMS intensities of typical secondary ions sputtered from the butane-adsorbed D_2O film as a function of temperature. 40 ML of the D_2O molecules were deposited on the Ni(111) substrate at 15 K and then heated at 100 K. 1 ML of C_4H_{10} molecules were adsorbed on it at 15 K. The temperature was increased at a rate of 5 K min^{-1} .

substrate was a Ni(111) surface, which was cleaned in the UHV chamber by heating to 1200 K using electron bombardment from behind. The D_2O , CH_3OH , and C_4H_{10} molecules were admitted into the UHV chamber through independent variable leak valves, and the molecules were adsorbed on the Ni(111) substrate by backfilling the UHV chamber. The coverage of the molecules was determined from the evolution curves of sputtered ion intensities as a function of exposure. The TOF-SIMS and TPD spectra were recorded every 30 s at a ramping speed of 5 K min^{-1} .

The RAIRS experiment was made in a separate UHV chamber with a base pressure of 3×10^{-8} Pa. The infrared absorption spectra were taken using a Fourier transform infrared (FTIR) spectrometer (FTS40A; Bio-Rad Laboratories, Inc.) equipped with a liquid-nitrogen-cooled mercury cadmium telluride detector. The IR beam was reflected from a gold film deposited on a mirror-finished Ni plate with a grazing angle of 5° . The substrate was cooled to 85 K using liquid nitrogen. The spectra were taken over the wave number range of $400\text{--}4000\text{ cm}^{-1}$ with an 8 cm^{-1} resolution. The temperature was increased at the same ramping speed as that used for TOF-SIMS and TPD, and 50 spectra were taken continually at temperatures of $90\text{--}200\text{ K}$. The OH stretching band was measured for the discussion of phase transition of ASW into ice Ic. However, precise assignment of the band is difficult because it is broadened considerably as a result of anharmonicity of the vibrations generated by extensive hydrogen bonding.^{18–21} The water films were deposited from the mixture of D_2O (5 mol %) in H_2O , thereby facilitating a study of the decoupled OD stretching band of HOD molecules that avoided this difficulty.¹⁷ For this HOD concentration, a narrow OD stretch band was observed because of the absence of OD-OD interactions.

III. EXPERIMENTAL RESULTS

Figure 1 shows TOF-SIMS intensities of typical secondary ions sputtered from a butane-adsorbed D_2O film as a function of temperature. A D_2O film with a thickness of 40 monolayers (ML) was deposited on the Ni(111) substrate at 15 K; they were then heated to 100 K. The C_4H_{10} molecules

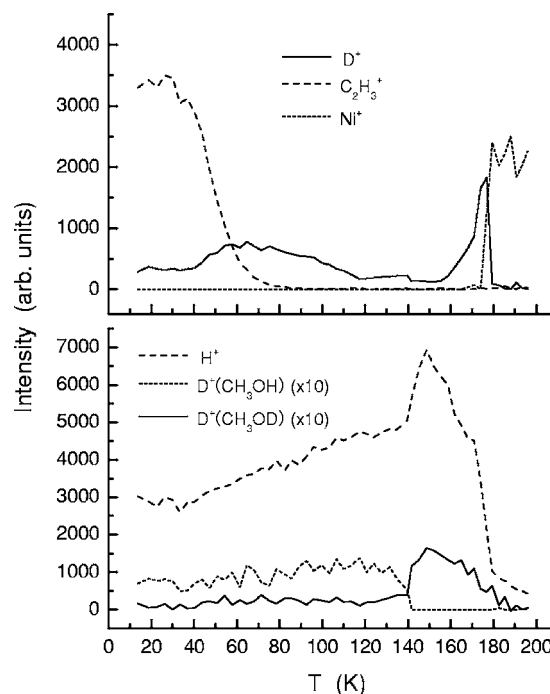


FIG. 2. TOF-SIMS intensities of typical secondary ions sputtered from the D_2O (40 ML) film coadsorbed with the C_4H_{10} (1 ML) and CH_3OH (2 ML) molecules as a function of temperature. The methanol-adsorbed D_2O film was preannealed up to 100 K, then butane was adsorbed on it at 15 K. The measurement was made at the same ramping speed as that in Fig. 1.

were adsorbed on the film after cooling to 15 K. The surface was covered with C_4H_{10} molecules, as confirmed from the sputtering of the $C_2H_3^+$ ions. At temperatures greater than 80 K, the C_4H_{10} molecules disappear completely from the surface. That disappearance results from dissolution of butane into the bulk of the D_2O film rather than desorption, as revealed from the TPD spectrum described later. The phenomenon is caused by pores or hydrogen-bond imperfections that are present in the ASW films.^{15,22} Consequently, ASW is sometimes regarded as a different material from HGW and LDA ice. However, the ASW film is known to relax to a material that is indistinguishable from HGW by annealing up to 113 K.²³ The Ni^+ ions evolve abruptly at 160–165 K because the D_2O film dewets the Ni(111) substrate. The D^+ ions come from the free OD group of the D_2O molecules at the surface, and they also drop in intensity at this temperature. These results suggest that a phase transition of water takes place at around 165 K prior to the film evaporation. Identical results are obtained for pure ASW films, indicating that butane has negligible effects on the properties of water described above.

Figure 2 shows similar experimental results for the methanol-adsorbed D_2O film. The CH_3OH molecules (2 ML) were adsorbed on the D_2O film (40 ML) at 15 K and then heated at 100 K. The C_4H_{10} molecules were adsorbed on it after cooling to 15 K. The butane dissolves in the film completely below 80 K, whereas the methanol generally remains on the D_2O film surface up to the film evaporation temperature, as revealed from the intensities of the H^+ - and

D^+ -attached methanol ions. The $D^+(CH_3OH)$ ion is the dominant molecular-ion species from methanol because ionization is caused by proton transfer from D_2O to CH_3OH during collisions. The absence of the $H^+(CH_3OH)$ ion shows that all the CH_3OH molecules form hydrogen bonds with the D_2O molecules during the preannealing process up to 100 K. Note that all the $D^+(CH_3OH)$ ions are converted to $D^+(CH_3OD)$ ions at temperatures greater than 140 K. The CH_3OD molecules are formed as a result of the H/D exchange between the hydroxyl groups of water and methanol; the attachment of the D^+ ion from D_2O to CH_3OD causes the $D^+(CH_3OD)$ ion. The H/D exchange is activated thermally, whereas the D^+ attachment is induced by the energetic collisions during sputtering. On the other hand, the H^+ ions are sputtered mainly from the CH_3 group. The H^+ intensity increases at temperatures greater than 140 K, suggesting that the methanol molecules change their orientation at this temperature. These behaviors are related to the glass-liquid transition of water because the self-diffusion and isotope scrambling of the water molecules commence at approximately 140 K.¹⁵ Another noticeable point is the absence of the hump in the sputtered Ni^+ intensity at 165 K, indicating that film dewetting is quenched by methanol. Some methanol molecules tend to desorb from the surface or dissolve in the bulk above 160 K, as revealed by the decrease (increase) of the H^+ and $D^+(CH_3OD)$ ions (the D^+ ion from D_2O). From these behaviors, we infer that the surfactant effect of methanol of reducing the surface tension is the main reason for quenching the morphological change of the fluidized water film.¹⁴

The crystallization of water has been discussed extensively on the basis of the drastic change in the TPD spectra.^{12,13} Figure 3(a) shows the TPD spectrum of D_2O (20 amu) from the C_4H_{10} (1 ML) adsorbed D_2O film (40 ML). The film was prepared similarly to that in Fig. 1. The desorption rate of the D_2O molecules decreases abruptly at around 160–165 K, where film dewetting occurs. This behavior has been explained as the abrupt crystallization of water because the desorption rate of water molecules from the crystalline ice is inferred to be orders of magnitude smaller than that from the amorphous water.¹² In reality, however, this phenomenon cannot be assigned uniquely to crystallization because the assumption of the layer-by-layer desorption from the uniform film surface is not valid for the pure ASW film. Figure 3(b) displays the TPD spectrum of D_2O from the methanol-adsorbed ASW film; the butane (1 ML) adsorbed D_2O film was annealed at 100 K, then methanol (2 ML) was adsorbed on it at 15 K. The hump in the D_2O TPD scan at 165 K disappears when methanol is present on the surface. The results therefore demonstrate that the hump is related to the change in film morphology.

The TPD spectra of butane (58 amu) taken simultaneously with those of D_2O in Figs. 3(a) and 3(b) are shown respectively in Figs. 4(a) and 4(b), together with the TPD spectrum of CH_3OD (32 amu for CH_2OD^+). The butane forms desorption peaks at temperatures greater than 110 K after being incorporated in the D_2O film at 80 K or higher temperatures (see Figs. 1 and 2). The first desorption peak at 117 K comes from the weakly bound butane molecules incorporated in the shallow subsurface site, whereas the peak

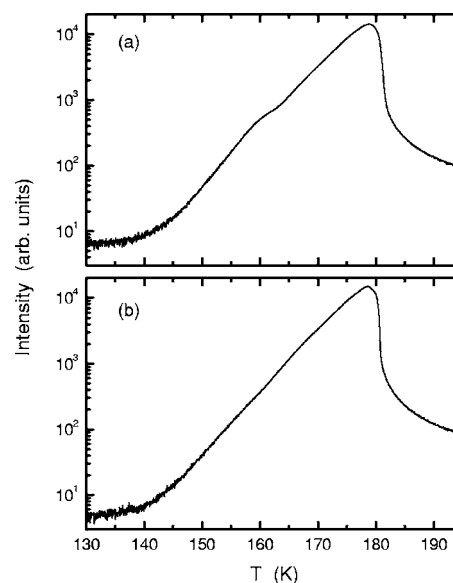


FIG. 3. TPD spectra of the D_2O molecules (20 amu) desorbed from the (a) C_4H_{10} (1 ML)/ D_2O (40 ML) and (b) CH_3OH (2 ML)/ C_4H_{10} (1 ML)/ D_2O (40 ML) films. The former was prepared in the same manner as that shown in Fig. 1, whereas the latter was prepared by preannealing of the butane-adsorbed D_2O film at 100 K, followed by deposition of methanol at 15 K. The spectra were taken at the same ramping speed as that shown in Fig. 1.

at 162 K in Fig. 4(a) is ascribable to hydrates of butane in the bulk. The high-temperature cutoff of the main peak (163 K) corresponds to the temperature for the simultaneous changes in the desorption rate of the D_2O molecules and the film morphology. According to the discussion of the explosive desorption of CCl_4 molecules embedded in the ASW

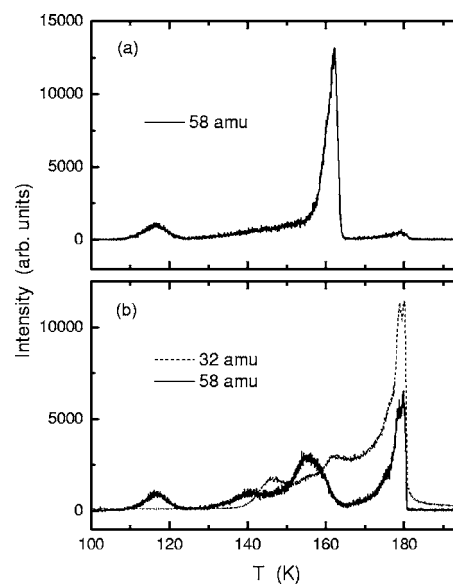


FIG. 4. TPD spectra of the C_4H_{10} (58 amu) and CH_3OD (32 amu for the CH_2OD^+ ion) molecules desorbed from (a) C_4H_{10} (1 ML)/ D_2O (40 ML) and (b) CH_3OH (2 ML)/ C_4H_{10} (1 ML)/ D_2O (40 ML). They were taken simultaneously with the D_2O TPD spectra shown in Figs. 3(a) and 3(b).

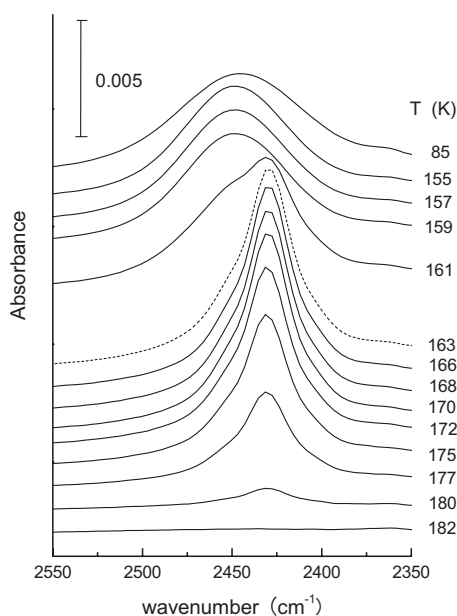


FIG. 5. RAIR spectra in the OD stretching region of HOD (10 mol %) in H_2O as a function of temperature. 40 ML of water molecules were deposited on the Au film at 85 K and the temperature was ramped at a rate of 5 K min^{-1} . The small structure at around 2350 cm^{-1} is attributable to uncompensated CO_2 .

films,¹³ the TPD peak of butane at 162 K should be related to the ASW film crystallization. However, the desorption kinetics of butane are strongly influenced by the methanol adsorbed on the surface, as shown in Fig. 4(b); the main peak at 162 K splits into two peaks at 155 and 180 K, and an additional peak emerges at 140 K. The TPD spectrum of methanol exhibits a broad structure, together with three peaks at 146, 162, and 180 K. The desorption kinetics of the butane and methanol molecules appears to be mutually correlated, as inferred from the alternative emergence of the peaks with increasing temperature.

Figure 5 shows the IR absorption band of the OD stretching vibration for 10 mol % HOD in the 40 ML H_2O film as a function of temperature. The band from the as-deposited film at 85 K exhibits a maximum at 2453 cm^{-1} ; the spectrum is changed very little by heating to 160 K. The band narrows and shifts to 2435 cm^{-1} at 163 K after film dewetting occurs. The redshift and narrowing of the spectra have been explained by crystallization.¹⁷ Consequently, this result shows that spontaneous nucleation occurs abruptly at temperatures near 160–165 K. The peak shape is not changed until the water film evaporates completely. It is noteworthy that the spectra after crystallization are asymmetric: the narrow peak at 2435 cm^{-1} is overlapped by a broader peak, as evidenced by the existence of a hump at around 2450 cm^{-1} and a tail toward the low-frequency side. Although the actual absorption band of ice Ic is not known, the overlapped broad peak is most likely to be caused by the contribution of the coexisting amorphous phase. In fact, a quite similar absorption band was observed in the FTIR spectra of HGW.¹⁷ It was explained by the overlapping of the crystalline and amorphous peaks. The present result shows that crystallization to ice Ic is not complete until the film evaporates if the sym-

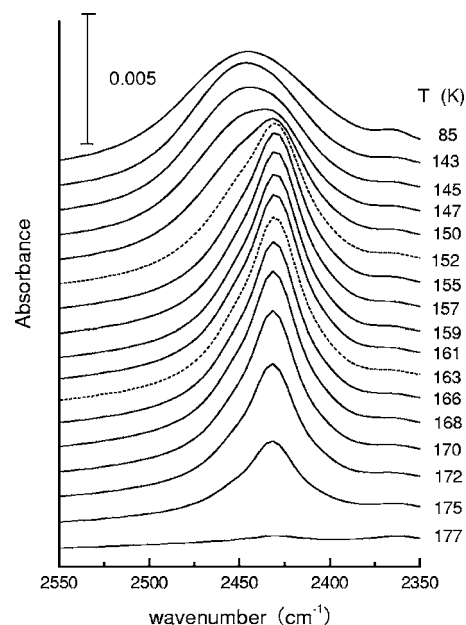


FIG. 6. Same as in Fig. 5, but 2 ML of methanol was adsorbed on 40 ML water film.

metric peak centered at 2435 cm^{-1} is assigned to the absorption band of crystals.¹⁷ The effect of the adsorbed butane or hexane on the IR band of the H_2O film was investigated (not shown), but the crystallization kinetics were not affected by the presence of these molecules.

Figure 6 displays the OD stretch band of HOD in the 40 ML H_2O film on which 2 ML of the CH_3OH molecules are adsorbed. In this case, the shape of the IR band changes at around 150 K because of the crystallization; no further changes in the band are observed at higher temperatures. The band is asymmetric, similar to that shown in Fig. 5, suggesting the coexistence of the crystal and amorphous phases. The lowering of the crystallization temperature is observed only when the multilayers of methanol are adsorbed: the crystallization temperature is fixed at around 152 K over the methanol coverage of 2–20 ML. The monolayer of methanol does not lower the crystallization temperature of water because it tends to stay at the surface as a surfactant. It is therefore inferred that the excess methanol molecules that are incorporated in the bulk play a role in lowering the crystallization temperature of the ASW film. This assumption may be supported by the fact that the adsorption of the other alcohols with a longer aliphatic chain, such as ethanol and 1-butanol, does not lower the crystallization temperature of water although they act as a surfactant to quench the film dewetting. The lower solubility of these alcohols in water is thought to be responsible for this behavior.

The crystallization temperature of 152 K observed in Fig. 6 agrees with that obtained in a calorimetric study for pure HGW films:^{5,6} the crystallization exotherm appears in a differential scanning calorimetry (DSC) output over a wide temperature range of 150–175 K. The crystallization of both pure and methanol-adsorbed ASW films occurs in a narrower temperature range (5–10 K) than in the calorimetric studies (20–25 K). This discrepancy might be ascribed to the kinetics because the DSC scan was made at a faster ramping

speed (30 K min^{-1}) than that used in this study (5 K min^{-1}). However, the crystallization temperature of 160–165 K for the pure ASW film is considerably higher than the crystallization onset of 152 K determined from the calorimetric study of the pure HGW film.^{5,6} This discrepancy is ascribable to the difference in the sample quality between the HGW and ASW films, as will be discussed later. The present results show that the kinetics of crystallization is affected strongly by the specific additives that are incorporated in the bulk of the water films.

IV. DISCUSSION

The presence of the two onsets for the liquidlike properties of water, i.e., the self-diffusion of the water molecules (136 K) and dewetting of the film (165 K), strongly suggests that the glass-liquid transition of water is a two-step process. Moreover, it is noteworthy that these two characteristic temperatures coincide with the conventional and reassigned T_g of water. The glass-transition temperature is definable as the onset of translational diffusion ($T_g=136 \text{ K}$), so that the following change in the nature of liquidlike water at around 165 K might be assigned to the liquid-liquid transition.¹⁶ For that reason, two liquidlike phases of water might exist in the deeply supercooled regime. In this regard, it is known that two distinct amorphous ices are present below T_g , as evidenced by discontinuous changes in specific volume and enthalpy between low-density and high-density forms of amorphous solid water (LDA and HDA, respectively).²⁴ The observed polymorphism between LDA and HDA might be extended to the supercooled liquid region. It is therefore hypothesized that a first-order liquid-liquid phase transition occurs between low-density liquid (LDL) and high-density liquid (HDL), and that their transition terminates at a second critical point that is located at around $T_{c'}=220 \text{ K}$ and $P_{c'}=100 \text{ MPa}$.^{1–4} According to this conjecture, liquidlike water in the deeply supercooled region should be categorized as a distinct LDL phase, whereas normal water consists of inseparable HDL and LDL domains. However, it is still unclear how amorphous water at low temperature is connected thermodynamically with normal liquid water under atmospheric pressure.²⁵

The liquid phase emerging at temperatures immediately higher than $T_g=136 \text{ K}$ may be LDL, which is characterized by an ultraviscous nature without exhibiting fluidity. The continuity of the hydrogen-bond structures between LDA (ASW) and LDL at 136 K is evidenced by the invariance of the IR absorption band (Fig. 5). LDL is a tetrahedrally structured liquid with strong, straight hydrogen bonds,²⁶ so that butane is thought to be incorporated in the cages of the water molecules. The incorporated butane molecules desorb almost completely at around 165 K. At this temperature, the hydrogen-bond structures of the water molecules change drastically, as evidenced by the dip in the TOF-SIMS D^+ intensity (Fig. 1), the change in the IR absorption band (Fig. 5), and the formation of aqueous LiCl solution.¹⁶ The high (poor) solubility of LiCl (butane) is characteristic of normal water, so that the liquid phase appearing above 165 K may be assigned to supercooled liquid water (LDL+HDL). Since

supercooled liquid water is unstable below the homogeneous nucleation temperature of 235 K, it crystallizes immediately into ice Ic at 165 K. For that reason, the IR absorption spectra exhibit the redshift due to crystallization rather than the blueshift expected from liquid water. The blueshifted IR band occurs when supercooled liquid water is quenched by the formation of a metastable LiCl solution, which is observed for the water/LiCl system.²⁷ Consequently, the drastic change in the properties of liquidlike water at around 165 K may be explained as the liquid-liquid transition (LDL \rightarrow LDL+HDL) that occurs prior to crystallization. After crystallization, another liquid phase appears to coexist with ice Ic, as revealed from the IR absorption results shown in Fig. 5: the broad peak overlapping with the sharp crystalline peak of ice Ic can be attributed to LDL. The coexisting liquid-like water may play a role in the progressive transformation of metastable ice Ic to hexagonal ice, Ih. Thus, water appears to become a material like a “molten sherbet” by heating to temperatures greater than 165 K. The liquidlike nature of water at temperatures of 140–220 K has been suggested from the diffraction and imaging studies by Jenniskens *et al.*¹⁸ By using transmission electron microscopy, they observed the formation of viscous droplets during crystallization of a 175 ML water film to ice Ic on an amorphous carbon surface. No crystallographic morphology expected from cubic ice was observed. The crystallization is inhibited when only 30% has transformed; most of the ice persists as a viscous liquid prior to crystallization to ice Ih.

A remarkable effect of adsorbed methanol is the lowering of the crystallization temperature from 165 to 152 K. This phenomenon is explainable by inducement via methanol of crystallization in the LDL phase, which is quenched for the pure water film. In this respect, two-stage crystallization is suggested in the calorimetric study of HGW:⁷ the crystallization rate increases at temperatures greater than 165 K after the onset at 152 K.^{5,6} The two-stage crystallization is explainable as resulting from the different crystal-growth rates of the LDL phase ($T < 165 \text{ K}$) and supercooled liquid water (LDL+HDL). It is likely that the crystal growth in the LDL phase is quenched without nuclei, whereas both spontaneous nucleation and nuclear growth occur in supercooled liquid water. No crystals are formed in the LDL phase of the ASW film because of the absence of nuclei. On the other hand, the HGW sample used in the calorimetric study was prepared by vitrification of aqueous aerosol droplets. It contains at least 5%–30% crystalline ice Ic depending on the cooling speed.²⁸ Consequently, the presence of nuclei and the crystal growth around them are thought to be responsible for crystallization in the LDL phase of the HGW film. In fact, we have confirmed that the crystallization temperature of the ASW film is lowered to 152 K provided that the ASW film is deposited on the crystalline (Ic) film that is formed by annealing the ASW film at 165 K.²⁷ In this context, the methanol incorporated in the bulk may induce the nucleation of water in the LDL phase, thereby enabling crystal growth at lower temperatures in the ASW film.

The methanol-induced crystallization also markedly influences the desorption kinetics of butane; the incorporated butane only partially desorbs during crystallization at 150–155 K, and a considerable amount of butane remains

until the evaporation temperature of the water film at 180 K. To date, it is considered that hydrophobes that are embedded in the thick water films desorb explosively due to crystallization because the molecules are released through cracks of crystal grains.¹³ For the pure ASW film shown in Fig. 4(a), however, butane is dehydrated at temperatures of 155–163 K before crystallization takes place. Therefore, we conclude that the dehydration is related to the phase transition of liquidlike water ($\text{LDL} \rightarrow \text{LDL} + \text{HDL}$) rather than crystallization ($\text{LDL} + \text{HDL} \rightarrow \text{LDL} + \text{Ic}$). If crystallization is induced in the LDL phase by the presence of methanol, butane can be incorporated in ice Ic without desorption, as inferred from the mutual similarity of the hydrogen-bond structures of LDA (LDL) and crystalline ice.²⁹ The incorporated butane in ice Ic is dehydrated at 180 K, together with the evaporation of the D_2O film.

With regard to the glass-liquid transition at 136 K, the related endotherm is so small that the precise assignment of T_g appears to be difficult in the calorimetric study.¹⁰ This result is quite reasonable because the glass-liquid transition ($\text{LDA} \rightarrow \text{LDL}$) is not a phase transition at all. On the other hand, a small endothermic hump, which is overlapped with a huge crystallization exotherm, is recognizable in the DSC output at around 165 K,^{5,6} although this behavior has been explained as the two-step crystallization, as mentioned previously.⁷ From comparison with the present result, this endothermic hump might be assigned to the first-order liquid-liquid phase transition ($\text{LDL} \rightarrow \text{LDL} + \text{HDL}$). The long relaxation time of glassy water attributable to the consecutive glass-liquid and liquid-liquid transitions is thought to be responsible for the confusion in the precise assignment of the calorimetric T_g value.

Recently, another point of confusion has arisen in relation to the crystallization of water. Kimmel *et al.* reported on the nonwetting growth of crystalline ice on a Pt(111) surface at 155 K by measuring the TPD of physisorbed Kr.³⁰ To date, the water monolayer on the Pt(111) surface has been considered to be similar to a bilayer plane from crystalline ice,^{31,32} so that the formation of droplets without epitaxial growth is ascribed to *hydrophobicity of the water monolayer*.³⁰ This assignment is misleading because nothing about the phase transition of liquidlike water is considered that occurs prior to crystallization. As discussed previously in the present paper, these two phenomena should be distinguished rigorously to avoid confusion. The dewetting behaviors of water are independent of the substrates and the presence or absence of the template water monolayer because the glass-liquid transition is a bulk phenomenon. This is confirmed from the fact that the water film with a moderate thickness (>20 ML) dewets the hydrophilic Ni(111) and hydrophobic graphite substrates at the same temperature.³³ The differences in the wettability of these substrates are observable in that the water monolayer remains on the Ni(111) substrate even after dewetting of the water film, whereas the dewetted patches of graphite above 165 K are molecularly clean. The Pt(111) substrate is identical to the Ni(111) substrate as far as the

dewetting behaviors of the water films are concerned (not shown). Therefore, the observed nonwetting growth of the crystalline ice on the Pt(111) surface is explicable simply by the occurrence of crystallization in the droplets of supercooled liquid water, leaving the ordered water monolayer on the dewetted patches of Pt(111). As a result, the assumption of the water monolayer hydrophobicity is not necessary. In fact, the wetted crystalline film may be grown if the crystallization occurs in the LDL phase, which is thought to be attainable by the preexisting nuclei. The monolayer of alcohols on the surface should also play a role in the wetting growth of the crystalline film because the surface tension of supercooled liquid water is reduced. In both cases, however, the film crystallinity is likely to be poor because of the coexistence of the amorphous phase.

V. CONCLUSION

The interactions between the ASW film and the coadsorbed butane and methanol molecules were investigated, and the kinetics of the glass-liquid transition and crystallization of water was discussed. Results showed that the liquidlike phase is dominant at temperatures of 136–165 K. The glass-liquid transition appears to occur in two steps: a distinct LDL phase emerges from LDA (ASW) at temperatures greater than 136 K, then the LDL phase transforms into supercooled liquid water ($\text{LDL} + \text{HDL}$) at approximately 165 K. The latter is thought to link directly to normal water, but it is only tentatively confirmed because crystallization occurs immediately. The crystallization in the LDL phase is characterized by nuclear growth, whereas both nucleation and nuclear growth occur in the supercooled liquid water ($\text{LDL} + \text{HDL}$). Crystallization in the LDL phase is thought to be quenched for the pure ASW film because of the absence of the nuclei. The butane may be incorporated in the cages of the hydrogen-bonded water molecules in the ASW film and is dehydrated almost completely during the liquid-liquid transition before the crystallization occurs at 165 K. Nothing happens for the incorporated butane during the glass-liquid transition at 136 K because of the continuity in the hydrogen-bond structures between LDA and LDL. On the other hand, the adsorbed methanol has a significant effect on the properties of the water film: the monolayer of methanol at the surface quenches dewetting because the surface tension of supercooled liquid water is reduced, and the methanol incorporated in the bulk induces nucleation of water in the LDL phase above 152 K. When the methanol-induced crystallization occurs, the butane molecules can be accommodated in the crystals, leading to the dehydration peak at 180 K. Therefore, almost complete dehydration of butane up to 165 K is related to the liquid-liquid transition rather than the crystallization. The crystallization of water is incomplete both with and without methanol, and ice Ic is inferred to be equilibrated with the viscous liquid phase (probably LDL), as evidenced by the overlapping of the broad IR absorption band.

- ¹P. H. Poole, F. Sciortino, U. Essmann, and H. E. Stanley, *Nature (London)* **360**, 324 (1992).
- ²O. Mishima and H. E. Stanley, *Nature (London)* **396**, 329 (1998).
- ³P. G. Debenedetti and H. E. Stanley, *Phys. Today* **56**(6), 40 (2003).
- ⁴P. G. Debenedetti, *J. Phys.: Condens. Matter* **15**, R1669 (2003).
- ⁵G. P. Johari, A. Hallbrucker, and E. Mayer, *Nature (London)* **330**, 552 (1987).
- ⁶G. P. Johari, A. Hallbrucker, and E. Mayer, *J. Chem. Phys.* **92**, 6742 (1990).
- ⁷G. P. Johari, *J. Chem. Phys.* **116**, 8067 (2002).
- ⁸V. Velikov, S. Borick, and C. A. Angell, *Science* **294**, 2335 (2001).
- ⁹Y. Yue and C. A. Angell, *Nature (London)* **427**, 717 (2004).
- ¹⁰N. Giovambattista, C. A. Angell, F. Sciortino, and H. E. Stanley, *Phys. Rev. Lett.* **93**, 047801 (2004).
- ¹¹A. Minoguchi, R. Richert, and C. A. Angell, *Phys. Rev. Lett.* **93**, 215703 (2004).
- ¹²R. S. Smith and B. D. Kay, *Nature (London)* **398**, 788 (1999).
- ¹³R. S. Smith, C. Huang, E. K. L. Wong, and B. D. Kay, *Phys. Rev. Lett.* **79**, 909 (1997).
- ¹⁴R. Souda, *Phys. Rev. Lett.* **93**, 235502 (2004).
- ¹⁵R. Souda, *J. Chem. Phys.* **121**, 8676 (2004).
- ¹⁶R. Souda, *J. Chem. Phys.* **125**, 181103 (2006).
- ¹⁷W. Hage, A. Hallbrucker, E. Mayer, and G. P. Johari, *J. Chem. Phys.* **100**, 2743 (1994).
- ¹⁸P. Jenniskens, S. F. Banham, D. F. Blake, and M. R. McCoustra, *J. Chem. Phys.* **107**, 1232 (1997).
- ¹⁹J. P. Devlin, C. Joyce, and V. Buch, *J. Phys. Chem. A* **104**, 1974 (2000).
- ²⁰E. H. G. Backus, M. L. Grecea, A. W. Kleyn, and M. Bonn, *Phys. Rev. Lett.* **92**, 236101 (2004).
- ²¹M. Ostblom, J. Ekeröth, P. Konradsson, and B. Liedberg, *J. Phys. Chem. B* **110**, 1695 (2006).
- ²²K. P. Stevenson, G. A. Kimmel, Z. Dohnalek, R. S. Smith, and B. D. Kay, *Science* **283**, 1505 (1999).
- ²³A. Hallbrucker, E. Mayer, and G. P. Johari, *J. Phys. Chem.* **93**, 4986 (1989).
- ²⁴O. Mishima, L. D. Calvert, and E. Whalley, *Nature (London)* **310**, 393 (1984).
- ²⁵R. J. Speedy, P. G. Debenedetti, R. S. Smith, C. Huang, and B. D. Kay, *J. Chem. Phys.* **105**, 240 (1996).
- ²⁶D. Paschek, *Phys. Rev. Lett.* **94**, 217802 (2005).
- ²⁷R. Souda (unpublished).
- ²⁸A. Hallbrucker and E. Mayer, *J. Phys. Chem.* **91**, 503 (1987).
- ²⁹J. L. Finney, A. Hallbrucker, I. Kohl, A. K. Soper, and D. T. Bowron, *Phys. Rev. Lett.* **88**, 225503 (2002).
- ³⁰G. A. Kimmel, N. G. Petrik, Z. Dohnalek, and B. D. Kay, *Phys. Rev. Lett.* **95**, 166102 (2005).
- ³¹A. Glebov, A. P. Graham, A. Menzel, and J. P. Toennies, *J. Chem. Phys.* **106**, 9382 (1997).
- ³²S. Haq, J. Harnett, and A. Hodgson, *Surf. Sci.* **505**, 171 (2002).
- ³³R. Souda, *J. Phys. Chem. B* **110**, 17524 (2006).